Syntheses and Electrochemistry of Sulfur-Bridged Incomplete Cubane-Type Mixed-Metal Clusters of Molybdenum(IV) and Tungsten(IV). X-ray Structures of $[MoW_2S_4(H_2O)_9](CH_3C_6H_4SO_3)_4\cdot 9H_2O$, $[Mo_2WS_4(H_2O)_9](CH_3C_6H_4SO_3)_4\cdot 9H_2O$, $Na_2[MoW_2S_4(Hnta)_3]\cdot 5H_2O$, and $Na_2[Mo_2WS_4(Hnta)_3]\cdot 5H_2O$

Takashi Shibahara,*,† Mikio Yamasaki,† Takayoshi Watase,† and Akio Ichimura‡

Departments of Chemistry, Okayama University of Science, 1-1 Ridai-cho, Okayama 700, Japan, and Faculty of Science, Osaka City University, Sugimoto, Sumiyoshi-ku, Osaka 558, Japan

Received June 4, 1993®

Reduction of a equimolar amount of $(NH_4)_2WS_4$ and $Na_2[Mo_2O_2S_2(cys)_2]\cdot 4H_2O$ with $NaBH_4$ gives a mixture of sulfur-bridged clusters, chromatographic separation of which gives novel incomplete cubane-type molybdenum-tungsten mixed-metal clusters $[MoW_2S_4(H_2O)_9]^{4+}$ and $[Mo_2WS_4(H_2O)_9]^{4+}$. From the aqua clusters solid samples $[MoW_2S_4(H_2O)_9](CH_3C_6H_4SO_3)_4\cdot 9H_2O$ (**MoW_2aq**) and $[Mo_2WS_4(H_2O)_9](CH_3C_6H_4SO_3)_4\cdot 9H_2O$ (**Mo_2Waq**) were isolated, and the derivatives $Na_2[MoW_2S_4(Hnta)_3]\cdot 5H_2O$ (**MoW_2nta**), and $Na_2[Mo_2WS_4(Hnta)_3]\cdot 5H_2O$ (**Mo_2Wnta**) were obtained (H_3nta = nitrilotriacetic acid). Crystal structures of the four clusters were determined. Compound **MoW_2aq** crystallized in the triclinic space group $P\bar{1}$ with a = 15.303(3) Å, b = 16.682(6) Å, c = 12.055(3) Å, α = 96.02(3)°, β = 108.58(2)°, γ = 102.16(2)°, V = 2802.1(15) Å^3, Z = 2, R = 4.77%. Compound **Mo_2Waq** crystallized in the triclinic space group $P\bar{1}$ with a = 15.327(5) Å, b = 16.704(5) Å, c = 12.057(5) Å, α = 95.64(3)°, β = 108.82(3)°, γ = 102.41(2)°, V = 2806.2(18) Å^3, Z = 2, R = 5.98%. Compound **MoW_2nta** crystallized in the monoclinic space group $P2_1/a$ with a = 21.754(5) Å, b = 12.733(5) Å, c = 13.374(5) Å, β = 101.95(3)°, V = 3624.4(21) Å^3, Z = 4, R = 3.90%. Compound **Mo_2Wnta** crystallized in the monoclinic space group $P2_1/a$ with a = 21.741(5) Å, b = 12.714(5) Å, c = 13.384(6) Å, β = 102.10(3), V = 3617.3(24) Å^3, Z = 4, R = 4.74%. Molybdenum and tungsten atoms in the four crystals are statistically disordered. Peak positions of the two big bands in each infrared spectrum of the four aqua clusters, $[Mo_3S_4(H_2O)_9](CH_3C_6H_4SO_3)_4\cdot 9H_2O$ (**Mo_3aq**), **Mo_2Waq**, **MoW_2aq**, and $[W_3S_4(H_2O)_9](CH_3C_6H_4SO_3)_4\cdot 9H_2O$ (**W_3aq**), in the 550–400-cm^{-1} region shift to lower wavenumbers when the molybdenum atom is replaced by tungsten. The bands are tentatively assigned to ν (metal–OH_2) (at higher wavenumber) and ν (metal$_3$–S) (at lower wavenumber). Binding energies of molybdenum ($3d_{3/2}$ and $3d_{5/2}$) and tungsten ($4f_{5/2}$ and $4f_{7/2}$) are obtained from XPS spectra of the clusters with $Mo_{3-n}W_nS_4$ cores (n = 0–3). The binding energies of Mo in **Mo_3aq** and **Mo_3nta** change little on the replacement of Mo with W, and those of W in **W_3aq** and **W_3nta** change little on the replacement of W with Mo, also: these phenomena can be explained by the softness of the bridging sulfurs, which act as a buffer for the electron density changes on the Mo and W atoms. Current-sampled dc polarograms and cyclic voltammograms of **MoW_2nta** and **Mo_2Wnta** show three consecutive one-electron reductive steps in alkaline solution (pH 11.4): $E_{1/2}$ (V vs Ag/AgCl) = –0.84, –1.40, –1.78; –0.73, –1.22, –1.66, respectively. These steps correspond to the change of oxidation states of the three metals in each cluster: (IV, IV, IV) → (IV, IV, III) → (IV, III, III) → (III, III, III). Electronic spectra of one-electron reduction products, the oxidation state being (IV, IV, III), obtained by bulk electrolysis of **MoW_2nta** and **Mo_2Wnta** have been reported for the first time. The half-wave potentials $E_{1/2}$ are significantly dependent on the cluster metals. In all the reduction processes the $[Mo_nW_{3-n}S_4(Hnta)_3]^{2-}$ clusters (n = 0–3) are easily reduced with the increase in the numbers of Mo(n) in the cluster. The proceeding reduction center of the molybdenum-tungsten mixed-metal clusters is mainly on the Mo atom(s) rather than W atom(s).

Introduction

Molybdenum sulfur compounds have attracted much attention, and a large number of sulfur-bridged molybdenum compounds have appeared.[1] Among them, many incomplete cubane-type sulfur-bridged molybdenum compounds with Mo_3S_4 cores[2] have been reported and some tungsten analogs with W_3S_4 cores[3] also studied. However, the number of triangular molybdenum–tungsten mixed-metal compounds are very limited,[4–7] and $[Mo_2WS_4(C_5(CH_3)_5)_3]$ reported by Wachter and co-workers[8] is the only cluster to have the molybdenum-tungsten mixed-metal core, though some mixed-metal clusters with incomplete cubane-type $M_2M'S_4$ cores (M = Mo or W; M′ = other metal) have been reported.[9,10]

We now report the syntheses, characterization, and X-ray structures of incomplete cubane-type molybdenum(IV)–tungsten(IV) mixed-metal aqua cluster compounds $[MoW_2S_4(H_2O)_9](CH_3C_6H_4SO_3)_4\cdot 9H_2O$ (**MoW_2aq**) and $[Mo_2WS_4(H_2O)_9](CH_3C_6H_4SO_3)_4\cdot 9H_2O$ (**Mo_2Waq**) and their derivatives $Na_2[MoW_2S_4(Hnta)_3]\cdot 5H_2O$ (**MoW_2nta**) and $Na_2[Mo_2WS_4(Hnta)_3]\cdot 5H_2O$ (**Mo_2Wnta**) (H_3nta = nitrilotriacetic acid). Recently we reported the syntheses and properties of the aqua ions $[Mo_3S_4(H_2O)_9]^{4+}$ (**Mo_{3aq}′**) and $[W_3S_4(H_2O)_9]^{4+}$ (**W_{3aq}′**),

† Okayama University of Science.
‡ Osaka City University.
® Abstract published in *Advance ACS Abstracts*, December 15, 1993.
(1) Some recently published reviews: (a) Shibahara, T. *Coord. Chem. Rev.* **1993**, *123*, 73–147. (b) Shibahara, T. *Adv. Inorg. Chem.* **1991**, *37*, 143–173. (c) Lee, S. C.; Holm, R. H. *Angew. Chem., Int. Ed. Engl.* **1990**, *29*, 840–856. (d) Young, C. G. *Coord. Chem. Rev.* **1989**, *96*, 89–251. (e) Harris, S. Polyhedron **1989**, *8*, 2843–2882. (f) Zanello, P. *Coord. Chem. Rev.* **1988**, *83*, 199–275. (g) Cannon, R. D.; White, R. P. *Prog. Inorg. Chem.* **1988**, *36*, 195–298. (h) Darensbourg, D. J.; Zalewski, D. J.; Sanchez, K. M.; Delord, T. *Inorg. Chem.* **1988**, *27*, 821–829.

0020-1669/94/1333-0292$04.50/0

Table 1. Crystallographic Data for $[MoW_2S_4(H_2O)_9](pts)_4 \cdot 9H_2O$ (**MoW_2aq**), $[Mo_2WS_4(H_2O)_9](pts)_4 \cdot 9H_2O$ (**Mo_2Waq**), $Na_2[MoW_2S_4(Hnta)_3] \cdot 5H_2O$ (**MoW_2nta**), and $Na_2[Mo_2WS_4(Hnta)_3] \cdot 5H_2O$ (**Mo_2Wnta**)

	MoW_2aq	**Mo_2Waq**	**MoW_2nta**	**Mo_2Wnta**
formula	$MOW_2S_8O_{30}C_{28}H_{64}$	$Mo_2WS_8O_{30}C_{28}H_{64}$	$MoW_2S_4Na_2O_{23}N_3C_{18}H_{31}$	$Mo_2WS_4Na_2O_{23}N_3C_{18}H_{31}$
fw	1600.97	1513.06	1295.33	1207.42
space group	$P\bar{1}$ (No. 2)	$P\bar{1}$ (No. 2)	$P2_1/a$ (No. 14)	$P2_1/a$ (No. 14)
a, Å	15.303(3)	15.327(5)	21.754(5)	21.741(5)
b, Å	16.682(6)	16.704(5)	12.733(5)	12.714(5)
c, Å	12.055(3)	12.057(5)	13.374(5)	13.384(6)
α, deg	96.02(3)	95.64(3)		
β, deg	108.58(2)	108.82(3)	101.95(3)	102.10(3)
γ, deg	102.16(2)	102.41(2)		
V, Å^3	2802.1(15)	2806.2(18)	3624.4(21)	3617.3(24)
Z	2	2	4	4
T, °C	18	18	18	18
λ(Mo Kα), Å	0.71073	0.71073	0.71073	0.71073
d_{obsd}, g/cm^3	1.89	1.79	2.34	2.19
d_{calcd}, g/cm^3	1.898	1.791	2.374	2.217
μ, cm^{-1}	47.7	28.8	71.4	42.4
R,[a] %	4.77	5.98	3.90	4.74
R_w,[b] %	6.70	6.32	5.61	7.24

[a] $R = \sum||F_o| - |F_c||/\sum F_o|$. [b] $R_w = [\sum w(|F_o| - |F_c|)^2/\sum w|F_o|^2]^{1/2}$; $w = 1/[(\sigma|F_o|)^2 + g|F_o|^2]$; g = 0.0004 for **MoW_2aq**, 0.0002 for **Mo_2Waq**, 0.0023 for **MoW_2nta**, and 0.0053 for **Mo_2Wnta**.

and their derivatives $[Mo_3S_4(Hnta)_3]^{2-}$ (**Mo_3nta′**) and $[W_3S_4(Hnta)_3]^{2-}$ (**W_3nta′**).[11]

Now we have a series of clusters having the cores

$$Mo_3S_4 \quad Mo_2WS_4 \quad MoW_2S_4 \quad W_3S_4$$

and we are able to investigate the interaction between molybdenum and tungsten and to compare the characters of the elements in the incomplete cubane-type clusters with $Mo_{3-n}W_nS_4$ cores (n = 0–3). A preliminary report on this topic has appeared.[12]

Experimental Section

Materials. *p*-Toluenesulfonic acid (HPTS) was used after recrystallization from water. Sodium borohydride, nitrilotriacetic acid, and tetraethylammonium chloride, as well as most other reagents, were commercial samples and were used as received. $(NH_4)_2MoS_4$,[13] $(NH_4)_2WS_4$,[13] $Na_2[Mo_2O_2S_2(cys)_2] \cdot 4H_2O$,[14] $K_2[W_2O_2S_2(cys)_2] \cdot 5H_2O$,[15] $(NH_4)_3MoCl_6$,[16] and $K_3[W_2Cl_9]$[17] were obtained by published procedures.

Syntheses of Compounds. $[MoW_2S_4(H_2O)_9]^{4+}$ (MoW_2aq′**) and $[Mo_2WS_4(H_2O)_9]^{4+}$ (**Mo_2Waq′**) Aqua Ions and $[MoW_2S_4(H_2O)_9](CH_3C_6H_4SO_3)_4 \cdot 9H_2O$ (**MoW_2aq**) and $[Mo_2WS_4(H_2O)_9](CH_3C_6H_4SO_3)_4 \cdot 9H_2O$ (**Mo_2Waq**).** $(NH_4)_2WS_4$ (3.00 g, 8.62 mmol) and the bis(μ-sulfido)(cysteinato)molybdenum(V) dimer $Na_2[Mo_2O_2S_2(cys)_2] \cdot 4H_2O$ (5.55 g, 8.62 mmol) were dissolved in water (150 mL), and small portions (ca. 2 mL each) of $NaBH_4$ (9.0 g, 0.24 mol in 60 mL of H_2O) and 6 M HCl (60 mL) were added alternately to the solution. Then, an additional amount (240 mL) of 6 M HCl was added to the solution, which was heated at above 90 °C for 5 h with introduction of an air stream. During heating, 1 M HCl was added occasionally to keep the volume of the solution constant (ca. 300 mL). The solution was cooled to room temperature and filtered by suction. The filtrate was subjected to Sephadex G-15 column chromatography (4.0 cm × 100 cm, 1 M HCl). The sixth **MoW_2aq′** (gray) and seventh **Mo_2Waq′** (green) bands were collected and concentrated by use of a cation exchanger, Dowex 50W-X2 (2 M HCl). Sephadex G-15 column chromatography (2.0 cm × 150 cm, 1 M HCl) was applied again for purification. This concentration–purification process was repeated again; yields of **MoW_2aq′** and **Mo_2aq′** (in solution) were 9% and 15%, respectively. Other bands collected were as follows: first, $Mo_4S_4^{5+}$(aq), green; second, $Mo_3O_2S_2^{4+}$(aq), gray; third, unknown, greenish yellow; fourth, unknown, yellowish green; fifth, Mo_3-

(2) References cited in ref 1 and some of the papers giving earlier references: (a) Shibahara, T.; Yamasaki, M.; Sakane, G.; Minami, K.; Yabuki, T.; Ichimura, A. *Inorg. Chem.* **1992**, *31*, 640–647. (b) Lin, X.-T.; Huang, J.-Q.; Huang, J.-L. *Chin. J. Chem.* **1992**, *10*, 34–39. (c) Liu, Q.-T.; Lu, J.-X.; Sykes, A. G. *Inorg. Chim. Acta* **1992**, *200*, 623–626. (d) Routledge, C. A.; Sykes, A. G. *J. Chem. Soc., Dalton. Trans.* **1992**, 325–329. (e) Fedin, V. P.; Sokolov, M. N.; Fedorov, V. Ye. *Inorg. Chim. Acta* **1991**, *179*, 35–40. (f) Cotton, F. A.; Kibala, P. A.; Miertschin, C. S. *Inorg. Chem.* **1991**, *30*, 548–553. (g) Hegetschweiler, K.; Keiler, T.; Amrein, W.; Schneider, W. *Inorg. Chem.* **1991**, *30*, 873–876. (h) Cotton, F. A.; Feng, X. *Inorg. Chem.* **1991**, *30*, 3666–3670. (i) Cheng, W.; Zhang, Q.; Huang, J.; Lu, Jaixi. *Polyhedron* **1990**, *9*, 1625–1631. (j) Lu, S.-F.; Huang, M.-D.; Huang, J.-Q.; Huang, Z.-X.; Huang, J.-L. *Acta Crystallogr., Sect. C* **1990**, *46*, 2036–2039. (k) Fedin, V. P.; Sokolov, M. N.; Miranov, Yu. V.; Kolesov, B. A.; Tkachev, S. V.; Fedorov, V. Ye. *Inorg. Chim. Acta* **1990**, *167*, 39–45. (l) Lu, S.-F.; Huang, J.-Q.; Huang, Z.-X.; Huang, J.-L.; Lu, J.-X. *Jiegou Huaxue* **1990**, *9*, 116–120. (m) Fedin, V. P.; Kolesov, B. A.; Mironov, Yu. V.; Fedorov, V. Ye. *Polyhedron* **1989**, *8*, 2419–2423. (n) Cheng, W.; Zhang, Q.; Huang, J.; Lu, J. *Polyhedron* **1989**, *8*, 2785–2789. (o) Cotton, F. A.; Kibala, P. A.; Matusz, M.; McCaleb, C. S.; San-dor, R. B. W. *Inorg. Chem.* **1989**, *28*, 2623–2630. (p) Huang, M. D.; Lu, S. F.; Huang, J. Q.; Huang, J. L. *Acta Chim. Sin.* **1989**, *47*, 121–127. (q) Cotton, F. A.; Llusar, R.; Eagle, C. T. *J. Am. Chem. Soc.* **1989**, *111*, 4332–4338. (r) Ooi, B.-L.; Sykes, A. G. *Inorg. Chem.* **1989**, *28*, 3799–3804. (s) Huang, J. Q.; Huang, J. L.; Shang, M. Y.; Lu, S. F.; Lin, X. T.; Lin, Y. H.; Huang, M. D.; Zhuang, H. H.; Lu, J. X. *Pure Appl. Chem.* **1988**, *60*, 1185–1192.

(3) References cited in refs 1 and 2, and some of the papers giving earlier references: (a) Cotton, F. A.; Mandal, S. K. *Inorg. Chim. Acta* **1992**, *192*, 71–79. (b) Fedin, V. P.; Sokolov, M. N.; Virovets, A. V.; Podberezskaya, N. V.; Fedorov, V. Y. *Polyhedron* **1992**, *11*, 853–855. (c) Fedin, V. P.; Sokolov, M. N.; Geras'ko, O. A.; Kolesov, B. A.; Fedorov, V. Ye.; Mironov, A. V.; Yufit, D. S.; Slovohotov, Yu. L.; Struchkov, Yu. T. *Inorg. Chim. Acta* **1990**, *175*, 217–229. (d) Naslerdin, M.; Olatunji, A.; Dimmock, P. W.; Sykes, A. G. *J. Chem. Soc., Dalton Trans.* **1990**, 1765–1769. (e) Zhan, H. Q.; Zheng, Y. F.; Wu, X. T.; Lu, J. X. *J. Mol. Struct.* **1989**, *196*, 241–247. (f) Zheng, Y. F.; Zhan, H. Q.; Wu, X. T. *Acta Crystallogr., Sect. C* **1989**, *45*, 1424–1426. (g) Fedin, V. P.; Sokolov, M. N.; Geras'ko, O. A.; Sheer, M.; Fedorov, V. Ye. *Inorg. Chim. Acta* **1989**, *165*, 25–26. (h) Cotton, F. A.; Llusar, R. *Inorg. Chem.* **1988**, *27*, 1303–1305.

(4) $[Mo_2W(\mu\text{-Br})_3(CO)_3(\eta\text{-Cp})_2(\mu_3\text{-}CC_6H_5)]$: Cotton, F. A.; Schwotzer, W. *Angew. Chem.* **1982**, *94*, 652–653.

(5) $[Mo_2W(\mu_3\text{-O})(\mu_3\text{-OR})(\mu\text{-OR})_3(OR)_6]$: Chisholm, M. H.; Folting, K.; Huffman, J. C.; Kober, E. M. *Inorg. Chem.* **1985**, *24*, 241–245.

(6) $[M_3(\mu_3\text{-O})_2(\mu\text{-}CH_3CO_2)_6(H_2O)_3]^{2+}$ (M_3 = Mo_2W and MoW_2): (a) Wang, B.; Sasaki, Y.; Nagasawa, A.; Ito, T. *J. Am. Chem. Soc.* **1986**, 6059–6060. (b) Wang, B.; Sasaki, Y.; Ikari, S.; Kimura, K.; Ito, T. *Chem. Lett.* **1987**, 1955–1958.

(7) $[Mo_2W(\mu_3\text{-O})(\mu\text{-O})_3(H_2O)_9]^{4+}$: Patel, A.; Richens, D. T. *J. Chem. Soc., Chem. Commun.* **1990**, 274–276.

(8) Brunner, H.; Kauermann, H.; Wachter, J. *J. Organomet. Chem.* **1984**, *265*, 189–198.

(9) M_2CuS_4: (a) Zhu, N.-Y.; Zheng, Y.-F.; Wu, X.-T. *Inorg. Chem.* **1990**, *29*, 2705–2707. (b) Zhu, N.-Y.; Zheng, Y.-F.; Wu, X.-T. *Polyhedron* **1991**, *10*, 2743–2755.

(10) M_2AgS_4: Zhu, N.-Y.; Wu, X.-T.; Lu, J.-X. *J. Chem. Soc., Chem. Commun.* **1991**, 235–237.

(11) Reference 2a and references cited therein.

(12) Shibahara, T.; Yamasaki, M. *Inorg. Chem.* **1991**, *30*, 1687–1688.

(13) McDonald, J. M.; Frisen, G. D.; Rosenheim, L. D.; Newton, W. E. *Inorg. Chim. Acta* **1983**, *72*, 205–210. Samples freshly prepared (or having been stored under dinitrogen atmosphere) should be used: Old samples will not dissolve in water and will therefore give lower yields.

(14) Shibahara, T.; Akashi, H. *Inorg. Synth.* **1992**, *29*, 254–260.

(15) Yamasaki, M.; Shibahara, T. *Inorg. Chim. Acta* **1993**, *205*, 45–51.

(16) Shibahara, T.; Yamasaki, M. *Inorg. Synth.* **1992**, *29*, 127–129.

(17) Saillant, R.; Hayden, J. L.; Wentworth, R. A. D. *Inorg. Chem.* **1967**, *6*, 1497–1501.

Table 2. Atomic Coordinates and Equivalent Isotropic Temperature Factors for $[MoW_2S_4(H_2O)_9](pts)_4 \cdot 9H_2O$ (**MoW_2aq**)[a]

atom	x	y	z	B_{eq}, Å^2
M1	0.71104(3)	0.10717(2)	0.11539(3)	2.60(1)
M2	0.67657(2)	−0.00755(2)	−0.08145(3)	2.16(1)
M3	0.73401(3)	−0.04894(2)	0.13783(4)	3.22(1)
S1	0.8252(1)	0.0518(1)	0.0677(2)	3.2(1)
S2	0.5763(1)	0.0699(1)	−0.0508(2)	2.9(1)
S3	0.6061(1)	−0.1229(1)	−0.0243(2)	3.3(1)
S4	0.6526(2)	0.0209(1)	0.2246(2)	3.4(1)
O11	0.6484(4)	0.1993(3)	0.1826(5)	3.6(2)
O12	0.7656(4)	0.2184(3)	0.0528(5)	4.1(2)
O13	0.8304(4)	0.1744(3)	0.2737(5)	3.7(2)
O21	0.5726(4)	−0.0608(4)	−0.2580(5)	3.7(2)
O22	0.7539(4)	−0.0754(4)	−0.1611(5)	4.5(2)
O23	0.7225(4)	0.0781(4)	−0.1892(5)	4.2(2)
O31	0.6938(5)	−0.1529(4)	0.2255(6)	5.5(2)
O32	0.8545(5)	−0.0201(5)	0.3012(6)	6.2(3)
O33	0.8243(5)	−0.1271(4)	0.1032(7)	6.2(3)
SP1	0.4362(2)	−0.2649(1)	−0.4382(2)	4.1(1)
SP2	0.5667(2)	0.3105(1)	−0.0634(2)	4.5(1)
SP3	1.0257(2)	0.2761(2)	0.1625(3)	7.1(1)
SP4	0.9376(3)	−0.2457(2)	0.3178(5)	8.6(2)
OP11	0.4585(5)	−0.2164(4)	−0.3206(5)	5.1(2)
OP12	0.3509(5)	−0.2503(5)	−0.5244(6)	6.2(3)
OP13	0.5158(5)	−0.2490(5)	−0.4797(7)	6.6(3)
OP21	0.6372(5)	0.2760(4)	−0.0973(6)	5.5(3)
OP22	0.5759(5)	0.3056(4)	0.0586(6)	5.3(3)
OP23	0.4703(6)	0.2749(5)	−0.1494(7)	7.4(3)
OP31	1.0958(6)	0.2363(6)	0.152(1)	9.8(5)
OP32	0.9389(5)	0.2529(5)	0.0511(7)	7.3(3)
OP33	0.9983(6)	0.2630(6)	0.2652(8)	8.7(4)
OP41	1.0365(8)	−0.2227(8)	0.329(1)	14.9(7)
OP42	0.891(1)	−0.240(1)	0.202(2)	21.(1)
OP43	0.905(2)	−0.2080(7)	0.391(2)	30.(2)
CP11	0.4087(6)	−0.3712(6)	−0.4281(8)	4.1(3)
CP12	0.386(2)	−0.4292(9)	−0.523(1)	12.4(9)
CP13	0.369(1)	−0.5135(9)	−0.515(1)	11.7(8)
CP14	0.3648(8)	−0.5421(7)	−0.418(1)	6.3(5)
CP15	0.376(2)	−0.484(1)	−0.333(2)	16.(1)
CP16	0.407(2)	−0.3957(8)	−0.329(1)	11.6(9)
CP17	0.335(1)	−0.6361(8)	−0.418(2)	10.5(8)
CP21	0.5983(6)	0.4178(5)	−0.0705(8)	3.9(3)
CP22	0.606(1)	0.4778(7)	0.018(1)	9.9(7)
CP23	0.636(1)	0.5620(7)	0.011(1)	8.4(6)
CP24	0.6490(8)	0.5870(6)	−0.080(1)	5.8(4)
CP25	0.636(2)	0.5247(9)	−0.168(2)	20.(2)
CP26	0.603(2)	0.4418(8)	−0.169(2)	19.(2)
CP27	0.674(1)	0.6791(7)	−0.085(2)	11.1(8)
CP31	1.0737(7)	0.3831(8)	0.175(1)	6.3(4)
CP32	1.091(2)	0.437(1)	0.271(1)	13.(1)
CP33	1.121(2)	0.520(1)	0.278(1)	12.(1)
CP34	1.1374(9)	0.5538(9)	0.190(1)	7.3(5)
CP35	1.129(3)	0.497(1)	0.100(2)	24.(2)
CP36	1.084(2)	0.411(1)	0.085(2)	20.(2)
CP37	1.173(1)	0.6497(9)	0.202(1)	9.5(7)
CP41	0.9095(7)	−0.3538(7)	0.320(1)	5.3(4)
CP42	0.919(1)	−0.3780(8)	0.423(1)	9.9(7)
CP43	0.893(2)	−0.4644(9)	0.422(1)	11.6(9)
CP44	0.8645(9)	−0.5231(8)	0.327(2)	7.4(5)
CP45	0.868(1)	−0.498(1)	0.228(2)	10.6(8)
CP46	0.890(1)	−0.409(1)	0.219(1)	11.4(9)
CP47	0.835(1)	−0.6170(8)	0.324(2)	13.(1)
OW1	0.6173(6)	0.1728(4)	−0.2960(6)	6.4(3)
OW2	0.9032(6)	0.1415(6)	−0.1577(7)	8.4(4)
OW3	0.4831(6)	0.0263(5)	−0.4015(7)	7.2(3)
OW4	0.8050(6)	0.2174(7)	0.4758(7)	9.2(4)
OW5	1.0341(6)	0.0170(7)	0.313(1)	11.1(5)
OW6	0.1320(8)	0.1809(7)	0.409(1)	11.9(5)
OW7	0.7013(7)	−0.1672(9)	−0.367(1)	15.3(6)
OW8	0.851(1)	0.0455(6)	0.5116(9)	13.6(6)
OW9A	0.916(1)	−0.100(1)	−0.033(1)	7.0(4)[b]
OW9B	0.936(1)	−0.039(1)	−0.121(1)	7.2(4)[b]

[a] Equivalent isotropic temperature factors ($B_{eq} = {}^4/_3\{\sum\sum \mathbf{B}_{ij} a_i a_j\}$). [b] Isotropic temperature factors were used. The following occupancy factors were used for the disordered atoms: OW9A, 0.5; OW9B, 0.5.

Table 3. Atomic Coordinates and Equivalent Isotropic Temperature Factors for $[Mo_2WS_4(H_2O)_9](pts)_4 \cdot 9H_2O$ (**Mo_2Waq**)[a]

atom	x	y	z	B_{eq}, Å^2
M1	0.7107(1)	0.1069(1)	0.1171(1)	3.54(3)
M2	0.67612(4)	−0.00717(4)	−0.0803(1)	2.28(3)
M3	0.7343(1)	−0.0491(1)	0.1397(1)	3.44(3)
S1	0.8241(2)	0.0518(2)	0.0702(3)	3.6(1)
S2	0.5753(2)	0.0687(2)	−0.0489(3)	3.4(1)
S3	0.6063(2)	−0.1223(2)	−0.0230(3)	3.9(1)
S4	0.6522(2)	0.0191(2)	0.2255(3)	4.0(1)
O11	0.6468(5)	0.1978(4)	0.1826(6)	3.8(3)
O12	0.7652(5)	0.2179(4)	0.0544(7)	3.9(3)
O13	0.8304(5)	0.1753(4)	0.2770(6)	3.9(3)
O21	0.5715(5)	−0.0618(5)	−0.2576(7)	4.1(3)
O22	0.7528(5)	−0.0738(5)	−0.1597(7)	5.0(3)
O23	0.7229(5)	0.0793(5)	−0.1891(7)	4.7(3)
O31	0.6951(6)	−0.1541(5)	0.2267(7)	5.5(3)
O32	0.8552(6)	−0.0187(5)	0.3086(8)	6.2(4)
O33	0.8243(6)	−0.1265(5)	0.1063(9)	6.7(4)
SP1	0.4383(2)	−0.2650(2)	−0.4383(3)	4.7(1)
SP2	0.5667(3)	0.3108(2)	−0.0624(3)	4.9(1)
SP3	1.0266(3)	0.2765(3)	0.1670(4)	7.0(2)
SP4	0.9416(4)	−0.2479(3)	0.3154(7)	9.9(3)
OP11	0.4614(6)	−0.2170(5)	−0.3219(8)	5.9(4)
OP12	0.3551(7)	−0.2511(6)	−0.5233(8)	7.3(4)
OP13	0.5189(6)	−0.2490(6)	−0.4773(8)	6.8(4)
OP21	0.6375(7)	0.2768(5)	−0.0962(8)	6.0(4)
OP22	0.5769(6)	0.3050(5)	0.0616(7)	5.8(4)
OP23	0.4707(7)	0.2769(6)	−0.1465(9)	8.1(4)
OP31	1.0966(8)	0.2355(7)	0.155(1)	11.4(7)
OP32	0.9417(7)	0.2502(6)	0.0575(9)	8.4(4)
OP33	0.9973(7)	0.2662(6)	0.2697(9)	7.8(4)
OP41	1.039(1)	−0.2240(8)	0.332(2)	16.4(9)
OP42	0.887(1)	−0.235(1)	0.216(2)	26.(1)
OP43	0.921(3)	−0.207(1)	0.406(3)	35.(3)
CP11	0.4089(8)	−0.3705(7)	−0.427(1)	4.3(4)
CP12	0.392(2)	−0.429(1)	−0.525(1)	12.(1)
CP13	0.366(2)	−0.515(1)	−0.513(2)	11.(1)
CP14	0.364(1)	−0.542(1)	−0.416(2)	7.1(8)
CP15	0.379(2)	−0.482(1)	−0.330(2)	15.(2)
CP16	0.407(2)	−0.397(1)	−0.329(2)	13.(1)
CP17	0.336(1)	−0.6356(9)	−0.416(2)	9.5(9)
CP21	0.5972(9)	0.4172(7)	−0.069(1)	4.1(5)
CP22	0.613(2)	0.478(1)	0.020(1)	9.6(9)
CP23	0.642(1)	0.563(1)	0.014(2)	9.1(9)
CP24	0.650(1)	0.586(1)	−0.080(2)	6.6(7)
CP25	0.628(2)	0.528(1)	−0.170(2)	17.(2)
CP26	0.605(2)	0.442(1)	−0.166(2)	16.(2)
CP27	0.678(1)	0.6795(8)	−0.081(2)	9.3(9)
CP31	1.0742(9)	0.384(1)	0.177(2)	6.4(6)
CP32	1.093(2)	0.440(1)	0.275(2)	13.(1)
CP33	1.125(2)	0.521(1)	0.278(2)	13.(1)
CP34	1.141(1)	0.555(1)	0.192(2)	7.0(7)
CP35	1.123(2)	0.499(2)	0.099(2)	21.(2)
CP36	1.084(3)	0.414(1)	0.083(2)	22.(2)
CP37	1.176(1)	0.6482(9)	0.202(2)	9.1(8)
CP41	0.9140(9)	−0.3528(9)	0.324(2)	5.5(6)
CP42	0.919(2)	−0.380(1)	0.423(1)	9.7(9)
CP43	0.892(2)	−0.465(1)	0.424(2)	11.(1)
CP44	0.864(1)	−0.523(1)	0.323(2)	7.4(8)
CP45	0.871(2)	−0.498(1)	0.228(2)	12.(1)
CP46	0.890(2)	−0.411(2)	0.220(2)	13.(1)
CP47	0.835(1)	−0.619(1)	0.327(2)	12.(1)
OW1	0.6124(7)	0.1719(5)	−0.2931(8)	7.1(4)
OW2	0.9023(6)	0.1446(7)	−0.1543(9)	8.3(5)
OW3	0.4820(7)	0.0252(6)	−0.4048(9)	8.3(5)
OW4	0.8014(8)	0.2170(8)	0.4786(8)	9.9(5)
OW5	1.0364(8)	0.0205(8)	0.317(1)	13.2(7)
OW6	0.1309(9)	0.182(1)	0.414(1)	15.4(8)
OW7	0.7047(8)	−0.171(1)	−0.356(1)	18.5(8)
OW8	0.854(1)	0.0466(7)	0.514(1)	14.6(7)
OW9A	0.923(1)	−0.099(1)	−0.028(2)	8.4(5)[b]
OW9B	0.942(2)	−0.035(2)	−0.119(2)	7.4(6)[b]

[a] Equivalent isotropic temperature factors ($B_{eq} = {}^4/_3\{\sum\sum \mathbf{B}_{ij} a_i a_j\}$). [b] Isotropic temperature factors were used. The following occupancy factors were used for the disordered atoms: OW9A, 0.6; OW9B, 0.4.

Table 4. Atomic Coordinates and Equivalent Isotropic Temperature Factors for $Na_2[MoW_2S_4(Hnta)_3]\cdot 5H_2O$ (**MoW_2nta**)[a]

atom	x	y	z	B_{eq}, Å^2
M1	0.09940(2)	0.50143(4)	0.29256(4)	1.07(3)
M2	0.08026(3)	0.70903(4)	0.24274(4)	1.50(3)
M3	0.17310(3)	0.59636(4)	0.17605(4)	1.18(3)
S1	0.1712(1)	0.6375(2)	0.3464(2)	1.7(1)
S2	0.0046(1)	0.5807(2)	0.2245(2)	1.8(1)
S3	0.0997(1)	0.7044(2)	0.0798(2)	1.8(1)
S4	0.1179(1)	0.4418(2)	0.1377(2)	1.7(1)
O11	0.0865(4)	0.5038(6)	0.4426(6)	2.0(2)
O12	0.1714(4)	0.3997(7)	0.3667(6)	2.0(2)
O13	0.0611(5)	0.4140(8)	0.5688(7)	3.6(3)
O14	0.2084(5)	0.2396(7)	0.3672(9)	4.0(3)
O15	−0.0252(5)	0.1533(8)	0.2920(8)	3.8(3)
O16	−0.0873(6)	0.212(1)	0.1502(8)	6.1(4)
O21	0.1284(4)	0.8559(6)	0.2665(6)	2.2(2)
O22	0.0530(4)	0.7689(7)	0.3744(6)	2.1(2)
O23	0.1292(4)	1.0238(7)	0.2234(7)	2.6(3)
O24	−0.0138(7)	0.863(1)	0.4393(9)	6.5(5)
O25	−0.0919(5)	0.9603(8)	0.0471(8)	3.5(3)
O26	−0.0968(5)	0.8401(8)	−0.0768(7)	4.0(3)
O31	0.2546(4)	0.5085(7)	0.2328(6)	2.0(2)
O32	0.2446(4)	0.7106(7)	0.1891(6)	2.4(2)
O33	0.3312(5)	0.409(1)	0.2010(9)	4.9(4)
O34	0.3176(5)	0.7848(8)	0.1198(8)	3.6(3)
O35	0.2390(4)	0.5481(9)	−0.1738(7)	3.3(3)
O36	0.1358(5)	0.544(1)	−0.2356(7)	3.8(3)
N1	0.0494(5)	0.3438(7)	0.3061(7)	1.6(3)
N2	0.0024(5)	0.8301(8)	0.1782(7)	1.9(3)
N3	0.2143(4)	0.5668(8)	0.0332(7)	1.6(3)
C11	0.0584(6)	0.427(1)	0.4788(9)	1.7(3)
C12	0.1646(6)	0.300(1)	0.3547(9)	2.2(3)
C13	0.0198(7)	0.355(1)	0.400(1)	2.6(4)
C14	0.0988(6)	0.259(1)	0.322(1)	2.7(4)
C15	−0.0017(6)	0.319(1)	0.216(1)	2.4(3)
C16	−0.0370(6)	0.219(1)	0.225(1)	2.6(4)
C21	0.1018(6)	0.9371(9)	0.220(1)	2.0(3)
C22	0.0062(7)	0.831(1)	0.367(1)	3.1(4)
C23	0.0372(6)	0.927(1)	0.154(1)	2.2(3)
C24	−0.0328(7)	0.851(1)	0.259(1)	2.8(4)
C25	−0.0404(6)	0.792(1)	0.082(1)	2.3(3)
C26	−0.0793(6)	0.876(1)	0.018(1)	2.2(3)
C31	0.2861(6)	0.464(1)	0.172(1)	2.4(3)
C32	0.2725(6)	0.7270(9)	0.115(1)	2.1(3)
C33	0.2618(7)	0.478(1)	0.057(1)	2.7(4)
C34	0.2468(6)	0.669(1)	0.015(1)	2.4(3)
C35	0.1640(6)	0.542(1)	−0.0604(9)	2.1(3)
C36	0.1853(6)	0.546(1)	−0.161(1)	2.3(4)
Na1	0.2263(3)	0.0656(5)	0.3417(5)	3.5(2)
Na2	0.2855(3)	0.4248(6)	0.4067(5)	4.6(2)
OW1	0.1652(5)	0.6039(8)	−0.4027(6)	2.8(3)
OW2	0.2316(6)	0.8995(9)	0.4237(9)	4.7(4)
OW3	−0.1255(5)	1.185(1)	0.4249(9)	4.8(4)
OW4	0.3300(8)	0.782(1)	0.371(1)	7.1(5)
OW5	0.3502(8)	0.575(1)	0.464(1)	9.0(7)

[a] Equivalent isotropic temperature factors ($B_{eq} = {}^4/_3\{\sum\sum \mathbf{B}_{ij}a_ia_j\}$).

OS_3^{4+}(aq), green; eighth, $Mo_3S_4^{4+}$(aq), green. The crystalline compounds **MoW_2aq** (black plate, yield 75% from **MoW_2aq′**) and **Mo_2Waq** (dark green plate, yield 74% from **Mo_2Waq′**) were prepared by a procedure similar to that for the synthesis of $[Mo_3S_4(H_2O)_9](CH_3C_6H_4SO_3)_4\cdot 9H_2O$ (**Mo_3aq**).[18] Anal. Found (calcd) for **MoW_2aq**: Mo, 5.7 (5.99); W, 23.2 (22.96); C, 21.38 (21.00); H, 3.35 (4.02). Anal. Found (calcd) for **Mo_2Waq**: Mo, 12.3 (12.68); W, 12.5 (12.15); C, 22.47 (22.22); H, 4.22 (4.26).

(18) Akashi, H.; Shibahara, T.; Kuroya, H. *Polyhedron* **1990**, *9*, 1671–1676.
(19) Katayama, C. *Acta Crystallogr., Sect. A* **1986**, *42*, 19–23.
(20) SHELXS-86: G. M. Sheldrick, Institute fuer Anorganische Chemie der Universitaet, Tammannstrasse 4, D-3400 Goettinggen, Federal Republic of Germany.
(21) *UNICS: The Universal Crystallographic Computation Program System*; The Crystallographic Society of Japan: Tokyo, 1969.
(22) C. K. Johnson, *ORTEP*; Report ORNL-3794; Oak Ridge National Laboratory: Oak Ridge, TN, 1965.
(23) (a) Reference 2a. (b) Yamasaki, M.; Shibahara, T. *Anal. Sci.* **1992**, *8*, 727–729. Not hepta- but pentahydrate is correct.

Table 5. Atomic Coordinates and Equivalent Isotropic Temperature Factors for $Na_2[Mo_2WS_4(Hnta)_3]\cdot 5H_2O$ (**Mo_2Wnta**)[a]

atom	x	y	z	B_{eq}, Å^2
M1	0.09945(4)	0.5005(1)	0.2932(1)	1.21(2)
M2	0.08015(4)	0.7087(1)	0.2432(1)	1.79(2)
M3	0.17315(4)	0.5957(1)	0.1763(1)	1.35(2)
S1	0.1709(1)	0.6370(3)	0.3462(2)	1.7(1)
S2	0.0053(2)	0.5802(3)	0.2247(2)	1.9(1)
S3	0.0993(2)	0.7030(3)	0.0809(2)	2.0(1)
S4	0.1177(2)	0.4418(3)	0.1383(2)	2.0(1)
O11	0.0864(4)	0.5039(7)	0.4447(7)	2.4(3)
O12	0.1714(4)	0.3980(7)	0.3666(7)	2.4(3)
O13	0.0615(6)	0.4122(9)	0.5698(8)	3.8(4)
O14	0.2079(5)	0.2388(9)	0.370(1)	4.2(4)
O15	−0.0258(5)	0.1531(9)	0.2930(8)	3.8(3)
O16	−0.0859(7)	0.211(1)	0.1494(9)	6.2(5)
O21	0.1278(4)	0.8557(7)	0.2664(7)	2.1(2)
O22	0.0532(4)	0.7691(8)	0.3744(7)	2.3(3)
O23	0.1297(4)	1.0235(7)	0.2236(8)	2.7(3)
O24	−0.0141(9)	0.866(1)	0.4374(9)	7.3(6)
O25	−0.0918(6)	0.9607(9)	0.0470(8)	3.8(3)
O26	−0.0979(6)	0.8401(9)	−0.0764(8)	4.2(4)
O31	0.2547(4)	0.5077(8)	0.2329(7)	2.2(3)
O32	0.2445(5)	0.7103(8)	0.1891(7)	2.5(3)
O33	0.3310(7)	0.409(1)	0.1997(9)	5.7(5)
O34	0.3177(5)	0.7839(9)	0.1188(8)	3.4(3)
O35	0.2386(5)	0.547(1)	−0.1737(8)	3.7(3)
O36	0.1360(5)	0.543(1)	−0.2361(7)	3.9(4)
N1	0.0477(5)	0.3427(8)	0.3071(8)	1.7(3)
N2	0.0031(5)	0.8298(9)	0.1790(8)	1.8(3)
N3	0.2136(5)	0.5672(9)	0.0328(8)	1.9(3)
C11	0.0585(7)	0.427(1)	0.478(1)	2.5(4)
C12	0.1646(6)	0.299(1)	0.355(1)	2.2(4)
C13	0.0190(8)	0.355(1)	0.400(1)	2.9(4)
C14	0.0980(6)	0.259(1)	0.322(1)	2.5(4)
C15	−0.0024(7)	0.318(1)	0.216(1)	2.5(4)
C16	−0.0369(7)	0.219(1)	0.226(1)	2.9(4)
C21	0.1033(7)	0.939(1)	0.220(1)	2.1(4)
C22	0.0054(8)	0.832(1)	0.366(1)	3.2(5)
C23	0.0374(7)	0.927(1)	0.154(1)	2.5(4)
C24	−0.0341(7)	0.851(1)	0.258(1)	2.8(4)
C25	−0.0399(7)	0.791(1)	0.081(1)	2.4(4)
C26	−0.0785(6)	0.875(1)	0.018(1)	2.4(4)
C31	0.2855(8)	0.464(1)	0.172(1)	3.5(5)
C32	0.2733(6)	0.726(1)	0.116(1)	2.1(4)
C33	0.2609(7)	0.479(1)	0.056(1)	2.5(4)
C34	0.2456(7)	0.670(1)	0.015(1)	2.5(4)
C35	0.1645(6)	0.539(1)	−0.0603(9)	2.4(4)
C36	0.1854(7)	0.543(1)	−0.161(1)	2.5(4)
Na1	0.2263(3)	0.0652(5)	0.3408(5)	4.0(2)
Na2	0.2849(4)	0.4227(7)	0.4062(6)	5.3(3)
OW1	0.1653(5)	0.6034(9)	−0.4014(7)	3.0(3)
OW2	0.2317(7)	0.900(1)	0.424(1)	5.2(4)
OW3	−0.1269(6)	1.185(1)	0.426(1)	5.1(4)
OW4	0.3298(8)	0.785(1)	0.370(1)	7.5(6)
OW5	0.349(1)	0.575(1)	0.462(2)	10.5(9)

[a] Equivalent isotropic temperature factors ($B_{eq} = {}^4/_3\{\sum\sum \mathbf{B}_{ij}a_ia_j\}$).

$Na_2[MoW_2S_4(Hnta)_3]\cdot 5H_2O$ (MoW_2nta**).** H_3nta (0.37 g, H_3nta/metal = 1.1) dissolved in a minimum amount of concentrated NaOH was added dropwise to a solution of the aqua trimer **Mo_2Waq′** (20 mL, 0.0290 M per trimer) in 1 M HCl, and the pH was adjusted to 1.2 with concentrated NaOH. The resulting precipitates were dissolved by heating the mixture above 90 °C with stirring in a water bath (ca. 30 min). Black rhombic crystals were obtained after storage in a refrigerator overnight and were collected by filtration, washed with ethanol, and air-dried; yield 0.63 g (84%). Anal. Found (calcd): N, 3.19 (3.24); C, 16.48 (16.69); H, 2.42 (2.41).

$Na_2[Mo_2WS_4(Hnta)_3]\cdot 5H_2O$ (Mo_2Wnta**).** A procedure similar to that used for the preparation of **MoW_2nta** was employed except for the use of **Mo_2Waq′** instead of **MoW_2aq′**. Typically, 20 mL of the aqua ion **Mo_2Waq′** (0.0438 M per trimer) in 1 M HCl and H_3nta (0.50 g) gave dark green rhombic crystals of **Mo_2Wnta**; yield 0.80 g (76%). Anal. Found (calcd): N, 3.38 (3.48); C, 17.40 (17.90); H, 2.70 (2.58).

Structural Determination of $[MoW_2S_4(H_2O)_9](CH_3C_6H_4SO_3)_4\cdot 9H_2O$ (MoW_2aq**), $[Mo_2WS_4(H_2O)_9](CH_3C_6H_4SO_3)_4\cdot 9H_2O$ (**Mo_2Waq**), Na_2-**

Table 6. Electronic Spectral Data for Trimers with $Mo_{3-n}W_nS_4$ (n = 0–3) Cores[a,b]

expt no.	compound	λ_{max}, nm(ϵ, M^{-1} cm^{-1})	ref
1	$[Mo_3S_4(H_2O)_9](pts)_4 \cdot 9H_2O$	367 (5190), 602 (351)	2a
2	$[Mo_2WS_4(H_2O)_9](pts)_4 \cdot 9H_2O$	345 (4900), 430 sh (914), 490 sh (298), 595 (322)	c
3	$[MoW_2S_4(H_2O)_9](pts)_4 \cdot 9H_2O$	327 (6200), 400 sh (1350), 490 (320), 568 (363)	c
4	$[W_3S_4(H_2O)_9](pts)_4 \cdot 9H_2O$	314 (7040), 430 sh (330), 560 (490)	2a
5	$K_2[Mo_3S_4(Hnta)_3] \cdot 9H_2O$	245 (21600), 379 (5900), 520 sh (330), 616 (463)	2a
6	$Na_2[Mo_2WS_4(Hnta)_3] \cdot 5H_2O$	245 sh (19200), 354 (5130), 420 sh (1500), 490 sh (410), 615 (420)	c
7	$Na_2[MoW_2S_4(Hnta)_3] \cdot 5H_2O$	235 sh (23300), 335 (5930), 400 sh (1630), 513 (412), 590 (460)	c
8	$Na_2[W_3S_4(Hnta)_3] \cdot 5H_2O$	220 (36200), 270 sh (7720), 320 (7090), 440 sh (440), 580 (730)	2a

[a] Data for experiments 1–4 in 2 M HPTS, for experiments 5–8 in water. [b] ϵ values per trimer. [c] This work.

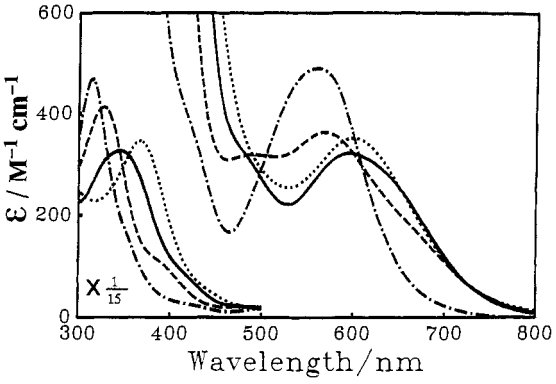

Figure 1. Electronic spectra of $[Mo_{3-n}W_nS_4(H_2O)_9]^{4+}$ clusters (n = 0–3) in 2 M HPTS: (···) $[Mo_3S_4(H_2O)_9]^{4+}$; (—) $[Mo_2WS_4(H_2O)_9]^{4+}$; (- -) $[MoW_2S_4(H_2O)_9]^{4+}$; (– · –) $[W_3S_4(H_2O)_9]^{4+}$.

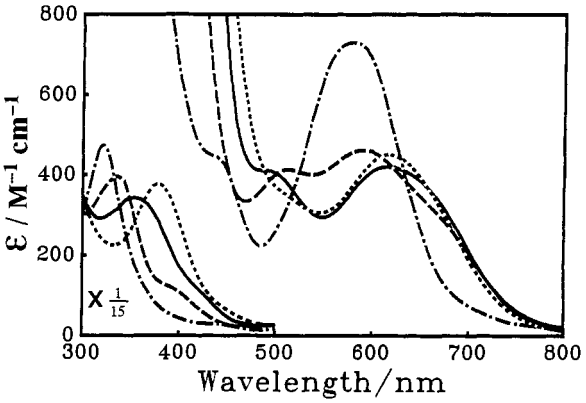

Figure 2. Electronic spectra of $[Mo_{3-n}W_nS_4(Hnta)_3]^{2-}$ clusters (n = 0–3) in water. (···) $[Mo_3S_4(Hnta)_3]^{2-}$; (—) $[Mo_2WS_4(Hnta)_3]^{2-}$; (- -) $[MoW_2S_4(Hnta)_3]^{2-}$; (– · –) $[W_3S_4(Hnta)_3]^{2-}$.

$[MoW_2S_4(Hnta)_3] \cdot 5H_2O$ (MoW_2nta), and $Na_2[Mo_2WS_4(Hnta)_3] \cdot 5H_2O$ (Mo_2Wnta). A black plate crystal (dimensions 0.33 × 0.29 × 0.29 mm) of **MoW_2aq** and a dark green plate crystal (dimensions 0.17 × 0.15 × 0.15 mm) of **Mo_2Waq** were mounted in glass capillaries, respectively, and a black rhombic crystal (dimensions 0.17 × 0.15 × 0.15 mm) of **MoW_2nta** and a dark green rhombic crystal (dimensions 0.17 × 0.15 × 0.15 mm) of **Mo_2Wnta** were mounted on glass fibers with an adhesive. The crystallographic and machine data for the four crystals are given in Table 1 and in the supplementary material (Table SI for **MoW_2aq**, Table SII for **Mo_2Waq**, Table SIII for **MoW_2nta**, and Table SIV for **Mo_2Wnta**). Systematic absences uniquely identified the space group as $P2_1/a$ for compounds **MoW_2nta** and **Mo_2Wnta**. Cell constants and orientation matrixes for the four crystals were obtained from least-squares refinement, by using setting angles of 25 reflections in the range 20° < 2θ < 30° measured on a Rigaku AFC-6A diffractometer by use of Mo Kα radiation (λ = 0.710 73 Å). The intensities of standard reflections monitored after every 150 reflections did not show any appreciable decay for the four crystals. Intensities were corrected for polarization and Lorentz factors. The corrections for absorption were applied to each crystal with the program CRYSTAN.[19] The same programs[19–22] that were used for the structure determination of **W_3aq**[2a] were used for the deduction of structures, refinement, and drawing of perspective views of **MoW_2aq**, **Mo_2Waq**, **MoW_2nta**, and **Mo_2Wnta**. No attempt was made to locate hydrogen atoms for each structural determination. Computations were performed on a FACOM M380 computer at the Okayama University of Science. The atomic coordinates and equivalent isotropic temperature factors of **MoW_2aq**, **Mo_2Waq**, **MoW_2nta**, and **Mo_2Wnta** are listed in Tables 2–5, respectively.

Electrochemical Measurements. Current-sampled dc polarography and cyclic voltammetry of the mixed-metal clusters **MoW_2nta**, and **Mo_2Wnta** were performed with the same instruments that were used for the measurements of $K_2[W_3S_4(Hnta)_3] \cdot 10H_2O$ and $K_2[Mo_3S_4(Hnta)_3] \cdot 9H_2O$.[2a] During the course of polarographic and voltammetric experiments, an argon atmosphere was maintained above the solution. Electrochemical measurements were performed at 25 ± 1 °C. HMDE was renewed before recording the voltammetric scans.

The pH of the sample solution (ca. 0.5 mM) containing 0.1 M KCl or 0.1 M tetraethylammonium chloride as supporting electrolyte was adjusted with 0.025 M borate buffer (pH 8.0–10.0), 0.025 M phosphate buffer (pH 10.9–11.5), or tetraethylammonium hydroxide (pH 11.0–12.0). All the solutions were deoxygenated with a stream of argon for at least 10 min prior to recording electrochemical data.

Other Measurements. UV, visible, and near-infrared spectra were recorded on a Hitachi 330, 320, or U2000 spectrophotometer. ICP spectrometry was applied for the analysis of molybdenum and tungsten using a Shimadzu ICPS-500 analyzer. Carbon, hydrogen, and nitrogen were determined by standard microanalytical procedures. Infrared spectra in Nujol mull were taken with a JEOL JIR-100 FT-IR spectrophotometer: measurements were repeated 100 times.

Scheme 1

$$(NH_4)_2WS_4 + Na_2[Mo_2O_2S_2(cys)_2] \cdot 5H_2O + NaBH_4 + HCl \rightarrow \mathbf{Mo_2Waq'} + \mathbf{MoW_2aq'} + \ldots$$

Results and Discussion

Syntheses and Properties of Molybdenum(IV)–Tungsten(IV) Mixed-Metal Clusters with MoW_2S_4 and Mo_2WS_4 Cores. We have tried two types of reactions for the syntheses of the mixed-metal clusters: type 1, reduction of a mixture of Mo(VI) (or Mo(V)) and W(VI) (or W(V)) compounds by $NaBH_4$; type 2 reduction of a mixture of Mo(VI) (or Mo(V)) and W(VI) (or W(V)) compounds by Mo(III) or W(III) compound. The method described in the Experimental Section employs a reaction of type 1 as described in Scheme 1. The combination of the starting materials gave better yields of **MoW_2aq'** and **Mo_2Waq'** than any other ones described below. The other combinations that we have tried so far were as follows: $(NH_4)_2MoS_4$, $K_2[W_2O_2S_2(cys)_2] \cdot 5H_2O$, $NaBH_4$; $K_2[W_2O_2S_2(cys)_2] \cdot 5H_2O$, $Na_2[Mo_2O_2S_2(cys)_2] \cdot 4H_2O$, $NaBH_4$; $(NH_4)_2WS_4$, $Na_2[Mo_2O_2S_2(cys)_2] \cdot 4H_2O$, $K_3[W_2Cl_9]$; $(NH_4)_2WS_4$, $Na_2[Mo_2O_2S_2(cys)_2] \cdot 4H_2O$, $(NH_4)_3MoCl_6$. The oxidation states of molybdenum and tungsten in the mixed-metal clusters are both four. The mixed-metal clusters are stable toward air oxidation: the absorption spectra of the clusters in 2 M HCl or freshly prepared 2 M HPTS solutions do not change for several days in the air.

It was demonstrated by the following two experiments that the clusters **MoW_2aq'** and **Mo_2Waq'** are *not* a mixture of $[Mo_3S_4(H_2O)_9]^{4+}$ and $[W_3S_4(H_2O)_9]^{4+}$: (1) The mixture of $[Mo_3S_4(H_2O)_9]^{4+}$ and $[W_3S_4(H_2O)_9]^{4+}$ is clearly separated into two bands by Sephadex G-15 column chromatography, while the **MoW_2aq'** (or **Mo_2Waq'**) cluster is not separated by the method. (2) The

electronic spectrum of the **MoW_2aq** cluster is clearly different from that of the mixture of 33% **Mo_3aq** and 66% **W_3aq** clusters. The same is true for **Mo_2Waq**. Elemental analyses and the agreement between calculated and observed densities for both the crystals also support the formulas.

The nitrilotriacetato derivatives of **MoW_2aq′** and **Mo_2Waq′**, **MoW_2nta** and **Mo_2Wnta**, respectively, were prepared at pH 1.2 in high yield as described in eq 1. The free carboxyl groups shown in structure **1** dissociate at higher pH's.

$$[Mo_2WS_4(H_2O)_9]^{4+} + 3H_3nta + 6NaOH \longrightarrow Na_2[Mo_2WS_4(Hnta)_3] + 15H_2O + 4Na^+ \quad (1)$$

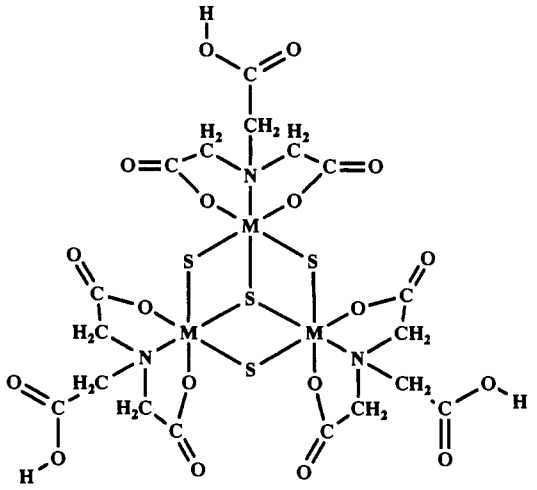

1

Electronic spectra of **MoW_2aq′** and **Mo_2Waq′** in the UV–visible region are shown in Figure 1 together with those of **Mo_3aq′** and **W_3aq′**. Corresponding spectra of $[Mo_nW_{3-n}S_4(Hnta)_3]^{2-}$ clusters (n = 0–3) are also depicted in Figure 2. No peaks were observed in the near-infrared region for all eight clusters. The peak positions (nm) and ϵ values are given in Table 6. Distinct splittings of absorption peaks in the visible region are observed in the mixed-metal aqua ions and the corresponding nta derivatives. The longer peak wavelength positions of the four aqua ions and of the four nta derivatives shift to longer wavelengths, respectively, when the tungsten atom is replaced by molybdenum. The peak positions of the aqua clusters and the nta derivatives in the 300–400-nm region also show the similar movements.

Structures of $[MoW_2S_4(H_2O)_9](CH_3C_6H_4SO_3)_4\cdot 9H_2O$ (MoW_2aq), $[Mo_2WS_4(H_2O)_9](CH_3C_6H_4SO_3)_4\cdot 9H_2O$ (Mo_2Waq), $Na_2[MoW_2S_4(Hnta)_3]\cdot 5H_2O$ (MoW_2nta), and $Na_2[Mo_2WS_4(Hnta)_3]\cdot 5H_2O$ (Mo_2Wnta). Molybdenum and tungsten atoms in the four crystals are statistically disordered, and the use of a weighted ((2Mo + W)/3) value of the atomic scattering factors of Mo^0 and W^0 gave reasonable temperature factors for the three metal atoms in **Mo_2Waq** and **Mo_2Wnta**, and another weighted value ((Mo + 2W)/3) is used satisfactorily for **MoW_2aq** and **MoW_2nta**. The four kinds of aqua crystals **MoW_2aq**, **Mo_2Waq**, $[W_3S_4(H_2O)_9](CH_3C_6H_4SO_3)_4\cdot 9H_2O$ (**W_3aq**),[2a] and $[Mo_3S_4(H_2O)_9](CH_3C_6H_4SO_3)_4\cdot 9H_2O$ (**Mo_3aq**)[18] are isomorphous with each other, and another isomorphous set of four crystals is **MoW_2nta**, **Mo_2Wnta**, $Na_2[Mo_3S_4(Hnta)_3]\cdot 5H_2O$[23] (**$Mo_3$nta**), and $Na_2[W_3S_4(Hnta)_3]\cdot 5H_2O$ (**W_3nta**).[2a] The structures of the cation of **MoW_2aq** and the anion of **MoW_2nta** are shown in Figures 3 and 4, respectively, and the selected interatomic distances and angles of **MoW_2aq**, **Mo_2Waq**, **MoW_2nta**, and **Mo_2Wnta** are collected in Tables 7–10, respectively. One uncoordinated CO_2 group in each $Hnta^{2-}$ ligand has a long distance (average 1.318[12] Å in **MoW_2nta**; 1.316[8]Å in **Mo_2Wnta**) and a short distance (1.208[17]Å in **MoW_2nta**; 1.210[4]Å in **Mo_2Wnta**), indicating

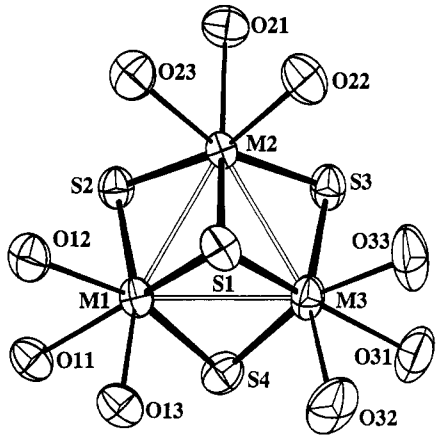

Figure 3. Perspective view of $[MoW_2S_4(H_2O)_9]^{4+}$ showing the atom-labeling scheme.

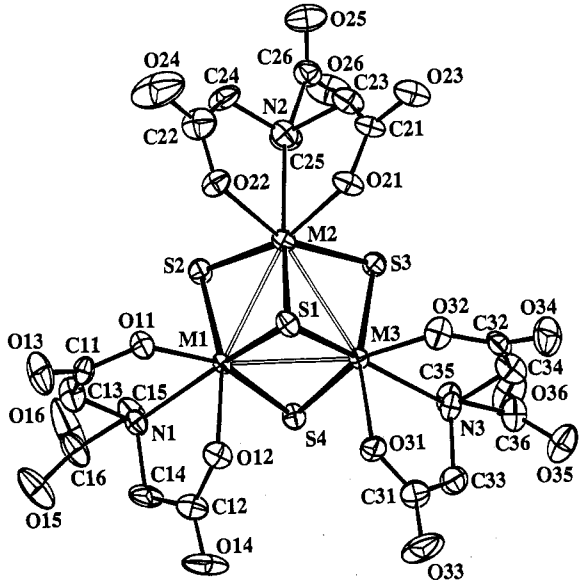

Figure 4. Perspective view of $[MoW_2S_4(Hnta)_3]^{2-}$ showing the atom-labeling scheme.

the existence of three –COOH groups in the each cluster anion as given in Tables 9 and 10. Comparison of bond distances (Å) in clusters with $Mo_{3-n}W_n$ cores (n = 0–3) are given in Table 11. A slight shortening of metal–metal distances was observed in both sets of the cluster compounds when molybdenum was replaced by tungsten.

XPS Spectra. Binding energies of molybdenum ($3d_{3/2}$ and $3d_{5/2}$) and tungsten ($4f_{5/2}$ and $4f_{7/2}$) are obtained from XPS spectra of the clusters with $Mo_{3-n}W_nS_4$ cores (n = 0–3) and are listed in Table 12. The binding energies of Mo in **Mo_3aq** and **Mo_3nta** do not change much on replacement of Mo with W, and those of W in **W_3aq** and **W_3nta** do not change much on replacement of W with Mo as well, which is in contrast to the case of $[M_3(\mu\text{-}O)_2(\mu\text{-}CH_3COO)_6(H_2O)_3]^{2+}$ ($M_3 = Mo_{3-n}W_n$ (n = 0–3)), where the binding energies of Mo in Mo_3 species decrease on replacement of Mo with W, and those of W in W_3 species increase on replacement of W with Mo.[6] The former have only bridging S atoms and terminal H_2O ligands whereas the latter have O, H_2O, and μ-CH_3COO groups, and no direct comparison can be made. However, the difference between the binding energy changes in the two types of clusters could be attributed to the softness of sulfur compared to oxygen: sulfur bridges work as a buffer for the electron density changes on the Mo and W atoms.

Infrared Spectra. Muller and co-workers extensively studied molybdenum-sulfur compounds and assigned the band of $(NH_4)_2[Mo_3(\mu_3\text{-}S)(\mu\text{-}S_2)_3(S_2)_3]$ at 460 cm^{-1} to $\nu(Mo_3\text{–}S)$—a vibration

Table 7. Selected Interatomic Distances (Å) and Angles (deg) in $[MoW_2S_4(H_2O)_9]^{4+}$

M1–M2	2.720(1)	M3–S4	2.279(3)
M1–M3	2.730(1)	mean	2.284[5]
M2–M3	2.719(1)	M1–O11	2.190(6)
mean	2.723[6]	M2–O21	2.168(5)
M1–S1	2.333(2)	M3–O31	2.202(7)
M2–S1	2.336(2)	mean	2.187[17]
M3–S1	2.356(2)	M1–O12	2.180(6)
mean	2.342[13]	M1–O13	2.169(4)
M1–S2	2.284(2)	M2–O22	2.160(8)
M1–S4	2.282(3)	M2–O23	2.183(7)
M2–S2	2.293(2)	M3–O32	2.150(6)
M2–S3	2.284(2)	M3–O33	2.190(8)
M3-S3	2.283(2)	mean	2.172[15]
M2–M1–M3	59.87(3)	O21–M2–O22	77.9(2)
M1–M2–M3	60.25(3)	O21–M2–O23	77.8(2)
M1–M3–M2	59.88(3)	O31–M3–O32	78.8(3)
mean	60.00[22]	O31–M3–O33	80.1(3)
S1–M1–S2	106.8(1)	mean	78.6[11]
S1–M1–S4	106.3(1)	O12–M1–O13	79.0(2)
S1–M2–S2	106.4(1)	O22–M2–O23	78.2(3)
S1–M2–S3	107.0(1)	O32–M3–O33	76.1(3)
S1–M3–S3	106.4(1)	mean	77.8[15]
S1–M3–S4	105.6(1)	M1–S1–M2	71.2(1)
mean	106.4[5]	M1–S1–M3	71.2(1)
S2–M1–S4	96.2(1)	M2–S1–M3	70.8(1)
S2–M2–S3	95.0(1)	mean	71.1[2]
S3–M3–S4	97.0(1)	M1–S2–M2	72.9(1)
mean	96.1[10]	M2–S3–M3	73.1(1)
O11–M1–O12	77.2(2)	M1–S4–M3	73.5(1)
O11–M1–O13	79.5(2)	mean	73.2[3]

Table 8. Selected Interatomic Distances (Å) and Angles (deg) in $[Mo_2WS_4(H_2O)_9]^{4+}$

M1–M2	2.727(2)	M3–S4	2.275(4)
M1–M3	2.734(1)	mean	2.283[7]
M2–M3	2.726(2)	M1–O11	2.188(8)
mean	2.729[4]	M2–O21	2.179(6)
M1–S1	2.326(4)	M3–O31	2.203(9)
M2–S1	2.332(3)	mean	2.190[12]
M3–S1	2.338(4)	M1–O12	2.175(8)
mean	2.332[6]	M1–O13	2.184(6)
M1–S2	2.285(3)	M2–O22	2.148(10)
M1–S4	2.287(4)	M2–O23	2.204(9)
M2–S2	2.293(4)	M3–O32	2.190(7)
M2–S3	2.275(3)	M3–O33	2.182(10)
M3–S3	2.281(3)	mean	2.181[19]
M2–M1–M3	59.88(4)	O21–M2–O22	77.4(3)
M1–M2–M3	60.19(4)	O21–M2–O23	78.2(3)
M1–M3–M2	59.93(4)	O31–M3–O32	78.5(3)
mean	60.00[17]	O31–M3–O33	79.3(4)
S1–M1–S2	106.7(1)	mean	78.4[9]
S1–M1–S4	105.7(1)	O12–M1–O13	78.8(3)
S1–M2–S2	106.2(1)	O22–M2–O23	77.7(3)
S1–M2–S3	106.5(1)	O32–M3–O33	77.2(3)
S1–M3–S3	106.1(1)	mean	77.9[8]
S1–M3–S4	105.7(1)	M1–S1–M2	71.7(1)
mean	106.2[4]	M1–S1–M3	71.8(1)
S2–M1–S4	95.6(1)	M2–S1–M3	71.4(1)
S2–M2–S3	94.5(1)	mean	71.6[2]
S3–M3–S4	96.7(1)	M1–S2–M2	73.1(1)
mean	95.6[11]	M2–S3–M3	73.5(1)
O11–M1–O12	77.4(3)	M1–S4–M3	73.7(1)
O11–M1–O13	79.6(3)	mean	73.4[3]

of the μ_3-S atom against the Mo_3 plane—[24] and the bands of $K_5[Mo_3S_4(CN)_9]\cdot 3KCN\cdot 4H_2O$ at 367 and 337 cm^{-1} to ν(Mo–S–Mo).[25] Fedin et al. also reported the infrared spectra of $(NH_4)_2[Mo_3S_{13}]\cdot 2H_2O$.[2m] Infrared spectra of the four aqua clusters, **Mo_3aq**, **Mo_2Waq**, **MoW_2aq**, and **W_3aq**, in 550–400-cm^{-1} region are shown in Figure 5. Each spectrum has two rather large absorption bands in the region. The peak positions shift to the lower wavenumbers when the molybdenum atom is replaced by the tungsten atom. The bands are tentatively assigned to ν(metal–OH_2) (at higher wavenumbers) and ν(metal$_3$–S) (at lower wavenumbers), and further investigation is necessary to get confirmed data.

Table 9. Selected Interatomic Distances (Å) and Angles (deg) in $[MoW_2S_4(Hnta)_3]^{2-}$

M1–M2	2.737(1)	M3–N3	2.303(10)
M1–M3	2.738(1)	mean	2.311[9]
M2–M3	2.771(1)	O11–C11	1.303(15)
mean	2.749[19]	O12–C12	1.279(15)
M1–S1	2.345(3)	O21–C21	1.282(14)
M2–S1	2.352(3)	O22–C22	1.273(18)
M3–S1	2.347(3)	O31–C31	1.291(17)
mean	2.348[4]	O32–C32	1.279(17)
M1–S2	2.307(3)	mean	1.285[11]
M1–S4	2.317(3)	O13–C11	1.203(15)
M2–S2	2.296(3)	O14–C12	1.213(16)
M2–S3	2.305(3)	O23–C21	1.252(14)
M3–S3	2.291(3)	O24–C22	1.217(21)
M3–S4	2.307(3)	O33–C31	1.209(17)
mean	2.304[9]	O34–C32	1.218(17)
M1–O11	2.083(9)	mean	1.219[17]
M1–O12	2.115(8)	O15–C16	1.220(16)
M2–O21	2.135(8)	O25–C26	1.189(17)
M2–O22	2.113(9)	O35–C36	1.215(17)
M3–O31	2.101(8)	mean	1.208[17]
M3–O32	2.110(9)	O16–C16	1.322(16)
mean	2.110[17]	O26–C26	1.327(16)
M1–N1	2.308(10)	O36–C36	1.305(14)
M2–N2	2.321(10)	mean	1.318[12]
M2–M1–M3	60.82(2)	O31–M3–O32	77.6(3)
M1–M2–M3	59.60(2)	mean	77.5[6]
M1–M3–M2	59.58(3)	O11–M1–N1	77.1(3)
mean	60.00[71]	O12–M1–N1	75.3(3)
S1–M1–S2	106.4(1)	O21–M2–N2	76.8(3)
S1–M1–S4	106.8(1)	O22–M2–N2	76.2(3)
S1–M2–S3	106.5(1)	O31–M3–N3	76.6(3)
S1–M2–S3	104.5(1)	O32–M3–N3	77.0(3)
S1–M3–S3	105.1(1)	mean	76.5[7]
S1–M3–S4	107.1(1)	M1–S1–M2	71.3(1)
mean	106.1[10]	M1–S1–M3	71.4(1)
S2–M1–S4	95.5(1)	M2–S1–M3	72.3(1)
S2–M2–S3	98.5(1)	mean	71.7[6]
S3–M3–S4	96.7(1)	M1–S2–M2	73.0(1)
mean	96.9[15]	M2–S3–M3	74.2(1)
O11–M1–O12	78.0(3)	M1–S4–M3	72.6(1)
O21–M2–O22	76.9(3)	mean	73.3[8]

Electrochemistry. Both of the molybdenum–tungsten mixed-metal clusters $[Mo_2WS_4(Hnta)_3]^{2-}$ (**Mo_2Wnta′**) and $[MoW_2S_4(Hnta)_3]^{2-}$ (**MoW_2nta′**) exhibit, as do $[Mo_3S_4(Hnta)_3]^{2-}$ (**Mo_3nta′**) and $[W_3S_4(Hnta)_3]^{2-}$ (**W_3nta′**),[2a] three reduction processes. Figure 6 shows a current-sampled dc polarogram (SP), a pulse polarogram (PP), and a cyclic voltammogram (CV) of **Mo_2Wnta′** at pH 11.4. Three consecutive reduction waves are observed in SP (Figure 6a) and PP (Figure 6b) although the wave height of the third reduction process is much larger than the equal height of the first and second waves in SP corresponding to the diffusion-limited current. A plot of E vs $\log((I_d - I)/I)$ gave a straight line with slopes of 66 and 69 mV for the first and second waves, respectively, indicating that both reductions are one-electron Nernstian processes corresponding to $[Mo_2WS_4(Hnta)_3]^{2-/3-/4-}$ redox couples. The third reduction process,

(24) (a) Muller, A.; Jostes, R.; Jaegermann, W.; Bhattacharyya, R. G. *Inorg. Chim. Acta* **1980**, *41*, 259–263. (b) Muller, A.; Wittneben, V.; Krickemeyer, E.; Bogge, H.; Lemke, M. *Z. Anorg. Allg. Chem.* **1991**, *605*, 175–188.

(25) Muller, A.; Reinsch, U. *Angew. Chem., Int. Ed. Engl.* **1980**, *19*, 72–73.

Table 10. Selected Interactomic Distances (Å) and Angles (deg) in $[Mo_2WS_4(Hnta)_3]^{2-}$

M1–M2	2.742(2)	M3–N3	2.303(12)
M1–M3	2.744(1)	mean	2.311[13]
M2–M3	2.777(1)	O11–C11	1.283(18)
mean	2.754[20]	O12–C12	1.267(17)
M1–S1	2.338(3)	O21–C21	1.281(16)
M2–S1	2.341(3)	O22–C22	1.299(20)
M3–S1	2.344(3)	O31–C31	1.283(21)
mean	2.341[3]	O32–C32	1.289(18)
M1–S2	2.296(3)	mean	1.284[10]
M1–S4	2.315(4)	O13–C11	1.229(18)
M2–S2	2.283(4)	O14–C12	1.200(18)
M2–S3	2.297(4)	O23–C21	1.219(17)
M3–S3	2.282(3)	O24–C22	1.210(23)
M3–S4	2.299(4)	O33–C31	1.201(22)
mean	2.295[12]	O34–C32	1.206(18)
M1–O11	2.105(10)	mean	1.211[11]
M1–O12	2.113(9)	O15–C16	1.214(18)
M2–O21	2.127(9)	O25–C26	1.210(19)
M2–O22	2.108(10)	O35–C36	1.207(20)
M3–O31	2.100(9)	mean	1.210[4]
M3–O32	2.108(10)	O16–C16	1.316(18)
mean	2.110[9]	O26–C26	1.324(18)
M1–N1	2.326(11)	O36–C36	1.309(16)
M2–N2	2.305(11)	mean	1.316[8]
S1–M1–S2	105.8(1)	O11–M1–N1	77.1(4)
S1–M1–S4	106.5(1)	O12–M1–N1	75.8(4)
S1–M2–S2	106.2(1)	O21–M2–N2	76.2(3)
S1–M2–S3	104.3(1)	O22–M2–N2	76.1(4)
S1–M3–S3	104.7(1)	O31–M3–N3	77.0(4)
S1–M3–S4	106.8(1)	O32–M3–N3	76.9(4)
mean	105.7[10]	mean	76.5[5]
S2–M1–S4	95.2(1)	M1–S1–M2	71.7(1)
S2–M2–S3	98.1(1)	M1–S1–M3	71.8(1)
S3–M3–S4	96.3(1)	M2–S1–M3	72.7(1)
mean	96.5[15]	mean	72.1[6]
O11–M1–O12	78.5(4)	M1–S2–M2	73.6(1)
O21–M2–O22	76.7(4)	M2–S3–M3	74.7(1)
O31–M3–O32	77.7(4)	M1–S4–M3	73.0(1)
mean	77.6[9]	mean	73.8[9]

which is considered to be a one-electron reduction, is accompanied by a catalytic reaction (EC′ mechanism[26]) involving H_2 evolution.[2a] The catalytic wave is significantly larger in SP compared to that in PP. This difference is interpreted in terms of the current-measuring time: 2.0 s in SP; 42 ms in PP. In CV at a hanging mercury drop electrode (Figure 6c), two electrochemically quasi-reversible and chemically reversible redox couples appear at −0.6 and −1.2 V,[27] respectively, although the third reduction peak disappears because of the very large catalytic H_2 evolution. Sharp redox peaks at −0.75 V due to the strong adsorption of **Mo_2Wnta′** on the mercury drop[28] overlap the peaks of the first reduction process. The adsorption peak corresponding to those in CV is also observed in PP.

Bulk controlled-potential coulometry of **Mo_2Wnta′** with a reticulated vitreous carbon electrode[29] at −1.1 V, which corresponds to the plateau part of the first reduction wave in SP and PP, confirms that the reduction is a one-electron process. Thus, the electrolysis yields the one-electron reduction product

(26) Bard, A. J.; Faulkner, L. R. *Electrochemical Methods*; Wiley: New York, 1980; p 455.

(27) Peak separations are as follows: Figure 6c, 280 (first), 150 mV (second); Figure 8c, 150 (first), 160 mV (second). The larger peak separation than the theoretical value expected for a reversible electrochemical process is affected by the strong adsorption on the stationary mercury electrode, while the continuous renewal of the electrode surface of the polarographic techniques used, especially sampled dc polarography, diminishes the adsorption.

(28) No peak due to the adsorption was observed in CV at a glassy-carbon electrode.

(29) No significant coulometric data was obtained using a mercury pool electrode because of the strong reactant and/or adsorption and the electrode mercury dissolution.

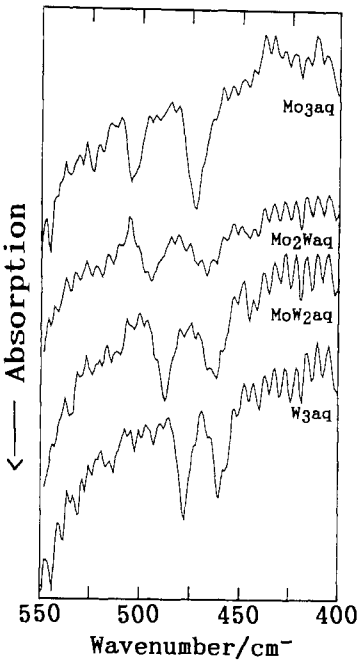

Figure 5. Infrared spectra of aqua clusters, $[Mo_3S_4(H_2O)_9](pts)_4\cdot 9H_2O$ (**Mo_3aq**), $[MoW_2S_4(H_2O)_9](pts)_4\cdot 9H_2O$ (**MoW_2aq**), $[Mo_2WS_4(H_2O)_9](pts)_4\cdot 9H_2O$ (**Mo_2Waq**), and $[W_3S_4(H_2O)_9](pts)_4\cdot 9H_2O$ (**W_3aq**) in the 550–440-cm^{-1} region.

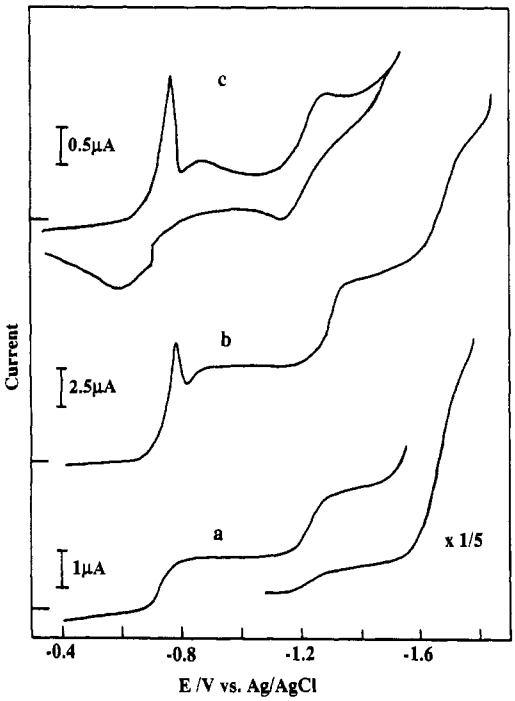

Figure 6. Electrochemical behavior of $[Mo_2WS_4(Hnta)_3]^{2-}$ (0.68 mM) in 0.1 M KCl at pH 11.4 with 0.025 phosphate buffer: (a) concurrent-sampled dc polarogram; (b) pulse polarogram; (c) cyclic voltammogram at a HMDE with a scan rate of 50 mV/s.

$[Mo_2WS_4(Hnta)_3]^{3-}$, which is stable in an inert atmosphere but is readily reoxidized to **Mo_2Wnta′** when exposed to air. The UV–visible spectra of the solution before and after the bulk electrolysis are shown in Figure 7. The reversible conversion of the spectra of the clusters was confirmed through several cycles of electrolytic reduction and air-oxidation, indicating the stability of the cores. The reduction product $[Mo_2WS_4(Hnta)_3]^{3-}$, which is a mixed-metal and mixed-valence cluster, has absorption maxima at 350, 610, and 780 nm.

As shown in Figure 8, the another molybdenum–tungsten mixed-metal cluster complex **MoW_2nta′** exhibits, as does **Mo_2-**

Table 11. Comparison of Bond Distances (Å) in Clusters with $Mo_{3-n}W_n$ Cores (n = 0–3)

compound	M–M	M–(μ_3-S)	M–(μ-S)	M–O	M–N	ref
$[Mo_3S_4(H_2O)_9](pts)_4 \cdot 9H_2O$	2.735[8]	2.337[5]	2.283[4]	2.18[1][a]		18
$[Mo_2WS_4(H_2O)_9](pts)_4 \cdot 9H_2O$	2.729[4]	2.332[6]	2.283[7]	2.18[2][a]		c
$[MoW_2S_4(H_2O)_9](pts)_4 \cdot 9H_2O$	2.723[6]	2.342[13]	2.284[5]	2.18[2][a]		c
$[W_3S_4(H_2O)_9](pts)_4 \cdot 9H_2O$	2.708[5]	2.338[8]	2.284[4]	2.17[2][a]		2a
$Na_2[Mo_3S_4(Hnta)_3] \cdot 5H_2O$	2.754[18]	2.334[4]	2.290[13]	2.112[16][b]	2.310[9]	23b
$Na_2[Mo_2WS_4(Hnta)_3] \cdot 5H_2O$	2.754[20]	2.341[3]	2.295[12]	2.110[9][b]	2.311[13]	c
$Na_2[MoW_2S_4(Hnta)_3] \cdot 5H_2O$	2.749[19]	2.348[4]	2.304[9]	2.110[17][b]	2.311[9]	c
$Na_2[W_3S_4(Hnta)_3] \cdot 5H_2O$	2.738[18]	2.349[2]	2.305[9]	2.102[16][b]	2.311[13]	2a

[a] Oxygen atom of water. [b] Oxygen atom of carboxylate group. [c] This work.

Table 12. Binding Energies(eV) of Clusters with $Mo_{3-n}W_n$ Cores (n = 0–3)[a]

compound	$Mo3d_{3/2}$	$Mo3d_{5/2}$	$W4f_{5/2}$	$W4f_{7/2}$	ref
$[Mo_3S_4(H_2O)_9](pts)_4 \cdot 9H_2O$	233.6	230.7			12
$[Mo_2WS_4(H_2O)_9](pts)_4 \cdot 9H_2O$	233.5	230.6	36.0	34.0	12
$[MoW_2S_4(H_2O)_9](pts)_4 \cdot 9H_2O$	233.4	230.5	35.9	33.8	12
$[W_3S_4(H_2O)_9](pts)_4 \cdot 9H_2O$			35.9	33.8	12
$Na_2[Mo_3S_4(Hnta)_3] \cdot 5H_2O$	233.2	230.1			b
$Na_2[Mo_2WS_4(Hnta)_3] \cdot 5H_2O$	233.1	230.0	35.6	33.4	b
$Na_2[MoW_2S_4(Hnta)_3] \cdot 5H_2O$	233.1	230.0	35.5	33.4	b
$Na_2[W_3S_4(Hnta)_3] \cdot 5H_2O$			36.1	34.0	b

[a] C_{1s} = 285.0 eV. [b] This work.

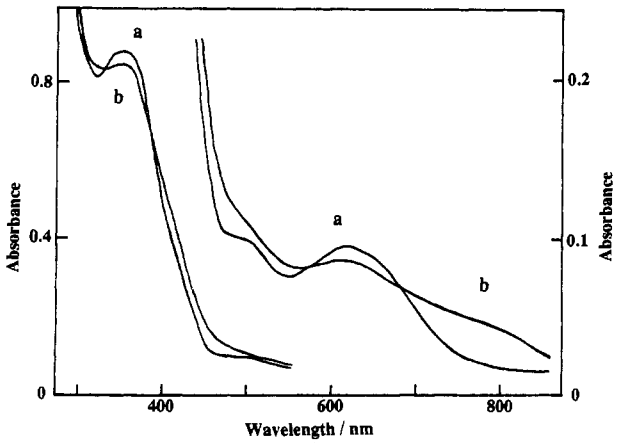

Figure 7. UV–visible spectra in 0.1 M KCl at PH 11.4: (a) $[Mo_2WS_4(Hnta)_3]^{2-}$ (0.19 mM); (b) the reduction product $[Mo_2WS_4(Hnta)_3]^{3-}$.

Wnta′, three consecutive one-electron reduction processes in the polarographic and voltammetric measurements although the third reduction wave accompanied with the catalytic H_2 evolution is too large in SP and CV at pH 11.4 to be separated from the background breakdown. The first reduction process at the mercury electrode is also overlapped by the adsorption redox couple at 0.7 V. Figure 9 shows UV–visible spectra of the solution before and after the controlled-potential electrolysis at −1.2 V. The electrolysis is coulometrically confirmed to be a one-electron reduction process to give the mixed-metal and mixed-valence cluster $[MoW_2S_4(Hnta)_3]^{3-}$ that has absorption maxima at 340, 580, and 720(sh) nm.

Table 13 summarizes the half-wave potentials and the wave slopes of the three consecutive one-electron reduction processes of the molybdenum–tungsten mixed-metal **Mo_2Wnta'** and **MoW_2nta'** clusters at pH 11.4 together with those of **Mo_3nta'** and **W_3nta'**.[30] The potential of the adsorption redox couple of the clusters on the mercury electrode is almost independent of the metals in the cluster, indicating that the specific interaction with Hg is through the sulfur atom in the clusters with the same order.[31] The catalytic H_2 evolution wave accompanying the third reduction process, however, depends markedly on the cluster; the catalytic reaction rate is in the order **W_3nta' > MoW_2nta' > Mo_2Wnta' > Mo_3nta'**,[32] while $E_{1/2}$ potentials for IV/III/III → III/III/III become less negative in the reverse order.

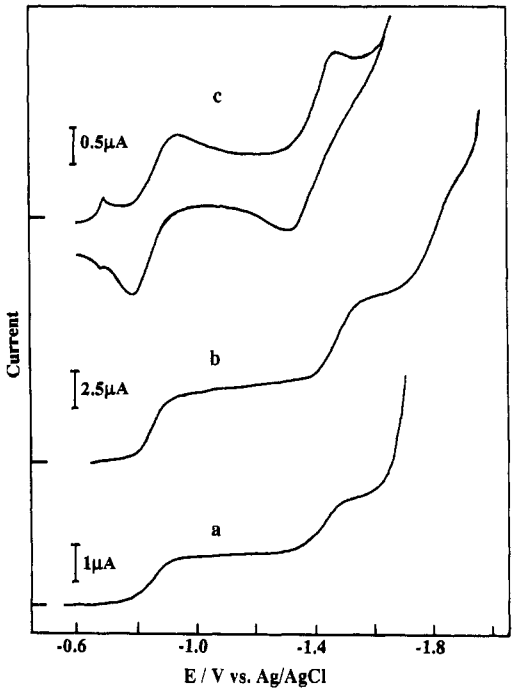

Figure 8. Electrochemical behavior of $[MoW_2S_4(Hnta)_3]^{2-}$ (0.62 mM) in 0.1 M KCl at pH 11.4 with 0.025 phosphate buffer: (a) concurrent-sampled dc polarogram; (b) pulse polarogram; (c) cyclic voltammogram at a HMDE with a scan rate of 50 mV/s.

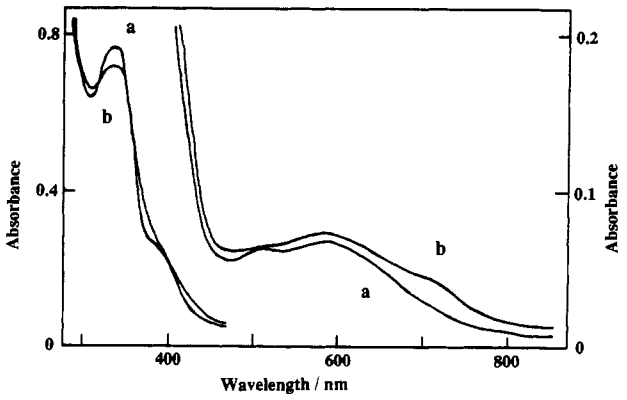

Figure 9. UV–visible spectra in 0.1 M KCl at PH 11.4: (a) $[MoW_2S_4(Hnta)_3]^{2-}$ (0.14 mM); (b) the reduction product $[MoW_2S_4(Hnta)_3]^{3-}$.

(30) We have observed the spectra of a series of $[Mo_{3-n}S_n(Hnta)_3]^{2-}$ (n = 0–4). The absorption maxima appreciably differ from each other. Similarity of the spectra of the mixed metal clusters in neutral and alkaline solution indicates no exchange of sulfur with oxygen in alkaline solution (pH 11.4). (For example: Shibahara, T.; Akashi, H.; Nagahata, S.; Hattori, H.; Kuroya, H. *Inorg. Chem.* **1989**, *28*, 362–370 and the references listed therein.)

(31) The adsorption redox couple appeared at −0.75 V is an adsorption prewave of the anodic mercury dissolution promoted by the clusters. An adsorption prewave is usually present in anodic polarograms of thiol compound. (Chambers, J. Q. In *Encyclopedia of Electrochemistry of Elements*; Bard, A. J., Lund, H., Eds.; Dekker: New York, 1978, Vol. XII-3.

Table 13. Comparison of $E_{1/2}$ for the Reduction of Clusters with $Mo_{3-n}W_n$ Cores (n = 0–3)[a,b]

	$E_{1/2}$ V vs Ag/AgCl			
	IV,IV,IV/ IV,IV,III	IV,IV,III/ IV,III,III	IV,III,III/ III,III,III	ref
$K_2[Mo_3S_4(Hnta)_3]\cdot 9H_2O$	−0.64 (70)	−1.08 (63)	−1.39[c]	2a
$Na_2[Mo_2WS_4(Hnta)_3]\cdot 5H_2O$	−0.73 (66)	−1.22 (69)	−1.66[c]	*d*
$Na_2[MoW_2S_4(Hnta)_3]\cdot 5H_2O$	−0.84 (59)	−1.40 (63)	−1.78[c]	*d*
$K_2[W_3S_4(Hnta)_3]\cdot 10H_2O$	−1.12 (59)	−1.41 (55)	−1.88[c]	2a

[a] Obtained from sampled dc polarogram. [b] Wave slopes (mV) are in parentheses. [c] Accompanied with the catalytic hydrogen wave. [d] This work.

The more interesting comparison is in the reduction potentials of the clusters. The reduction potentials represented by the half-wave potentials are significantly dependent on the cluster metals. In all the reduction processes the $[Mo_nW_{3-n}S_4(Hnta)_3]^{2-}$ clusters (n = 0–3) are easily reduced with the increase in the numbers of Mo(n) in the cluster. The reduction potentials of the mixed-metal clusters lie between those of **Mo₃nta′** and **W₃nta′** but are not proportionally distributed. For the first reduction process, the potential difference between $[MoW_2S_4(Hnta)_3]^{2-/3-}$ and $[W_3S_4(Hnta)_3]^{2-/3-}$ is 720 mV, which is markedly larger than that between $[Mo_3S_4(Hnta)_3]^{2-/3-}$ and $[Mo_2WS_4(Hnta)_3]^{2-/3-}$ (90 mV) and that between $[Mo_2WS_4(Hnta)_3]^{2-/3-}$ and $[MoW_2S_4(Hnta)_3]^{2-/3-}$ (110 mV). The largest potential difference for the second and third processes lies between $[Mo_2WS_4(Hnta)_3]^{3-/4-}$ and $[MoW_2S_4(Hnta)_3]^{3-/4-}$, and $[MoW_2S_4(Hnta)_3]^{4-/5-}$ and $[W_3S_4(Hnta)_3]^{4-/5-}$, respectively. These results suggest that the proceeding reduction center of the molybdenum–tungsten mixed-metal clusters is mainly on the Mo atom(s) rather than the W atom(s). Thus, the electrode reactions are formally described as

$$Mo^{IV}Mo^{IV}W^{IV} \xrightarrow{e^-} Mo^{III}Mo^{IV}W^{IV} \xrightarrow{e^-} Mo^{III}Mo^{III}W^{IV} \xrightarrow{e^-} Mo^{III}Mo^{III}W^{III}$$

and

$$Mo^{IV}W^{IV}W^{IV} \xrightarrow{e^-} Mo^{III}W^{IV}W^{IV} \xrightarrow{e^-} Mo^{III}W^{III}W^{IV} \xrightarrow{e^-} Mo^{III}W^{III}W^{III}$$

The spectroscopic measurements involving electron paramagnetic resonance spectroscopy may help us to elucidate in more detail electronic states of the reduced clusters, especially the mixed-metal and mixed-valence clusters.

Acknowledgment. This work was partly supported by a Grant-in-Aid for Scientific Research (No. 62470043, 02453043) from the Ministry of Education, Science and Culture of Japan. We are grateful to Prof. S. Kittaka of Okayama University of Science for the measurement of the infrared spectra.

Supplementary Material Available: Listings of crystallographic data, thermal parameters, bond distances and angles (Tables SI-SXV) (28 pages). Ordering information is given on any current masthead page.

(32) The order of the catalytic H_2 evolution rates was qualitatively estimated by comparing the ratios of the third catalytic wave height (catalytic) to the first wave height (diffusion-controlled). Background breakdown (H_2 evolution) of the solution at pH 11.4 without clusters appears at ca. −1.9 V, which is more negative than the half-wave potentials of the mixed metal clusters.